Structural Engineering and Mechanics, Vol. 4, No. 5 (1996) 469-484
DOI: http://dx.doi.org/10.12989/sem.1996.4.5.469

Closed-form Green's functions for transversely isotropic bi-solids with a slipping interface

Zhong Qi Yue†

Infrastructure Laboratory, Institute for Research in Construction, National Research Council of Canada, Ottawa, Ontario, K1A 0R6 Canada

Abstract. Green's functions are obtained in exact closed-forms for the elastic fields in bi-material elastic solids with slipping interface and differing transversely isotropic properties induced by concentrated point and ring force vectors. For the concentrated point force vector, the Green functions are expressed in terms of elementary harmonic functions. For the concentrated ring force vector, the Green functions are expressed in terms of the complete elliptic integral. Numerical results are presented to illustrate the effect of anisotropic bi-material properties on the transmission of normal contact stress and the discontinuity of lateral displacements at the slipping interface. The closed-form Green's functions are systematically presented in matrix forms which can be easily implemented in numerical schemes such as boundary element methods to solve elastic problems in computational mechanics.

Key words: bi-materials; closed-form solutions; elasticity; Green's functions; integral transforms; point body forces; ring body forces; slipping interface; transversely isotropic solids.

1. Introduction

Green's functions are introduced to represent the distribution of displacements and stresses in an elastic solid due to the action of concentrated forces prescribed either at the boundary surface or in the solid interior. Closed-form Green's functions are the peculiar ones which can be expressed in terms of elementary or special functions whose mathematical characteristics are well known. The main motivation of seeking Green's functions in elasticity originates from the fact that Green's functions can be employed to construct solutions for many problems of practical importance by using various analytical and numerical methods including eigenstrain, dislocation methods, boundary integral equations and boundary element methods (see, e.g., Elliott 1948, Mura 1982, Hasegawa and Kondou 1987, Lin and Keer 1989, Hanson 1992).

The objective of this paper is to present Green's functions in exact closed-form for elastic field in bi-material solids by taking into account the influences of slipping interface and transversely isotropic material properties. At a bi-material interface, slipping generally occurs when the interface shear stress reaches a limiting value based on a frictional law of Mohr-Coulomb type. There are many mathematical difficulties to consider such a more realistic situation of frictional bi-material interface. This paper considers a simplified and idealized situation of imperfect interface where the interface shear stress is assumed to be zero. Such idealized model of a slipping interface provides a mathematical convenience to obtain closed-form solutions of the Green's

† Research Associate

functions in bi-material solids and is a limiting case of the general frictional interface following Mohr-Coulomb type law. In some bi-material problems, the interface between the two materials fails in shear at relatively low shear stresses while a complete material contact is maintained (Dundurs and Stippes 1970). Such situations can arise in geotechnical engineering, bioengineering or composite materials (see, e.g., Gladwell and Hara 1981, Gharpuray *et al.* 1991, Selvadurai 1994, Wijeyewickrema and Keer 1994). For instance, a precompressed slipping bi-material interface was used by Gladwell and Hara (1981) and Selvadurai (1994) to examine unilateral contact problems in geomechanics.

Classical studies of the relevant elastic problems were given by Dundurs and Hetenyi (1965) who derived Green's functions for point forces parallel to, and perpendicular to the slipping contact interface between two dissimilar isotropic semi-infinite solids using the Papkovich-Neuber displacement functions. These closed-from results were used by Yuuki *et al.* (1987) to formulate boundary element methods for efficient elastostatic analysis. Pan and Chou (1979) obtained closed-form Green's functions for point force perpendicular to the slipping contact interface of two transveresly isotropic elastic halfspaces using potential function technique. More recently, using the method of images, Vijayakumar and Cormack (1987a) have extended the closed-form results to cover Green's functions for isotropic bi-material elastic solids with slipping interface subjected to nuclei of strain. Further studies related to closed-form Green's functions for bi-material elastic solids were given by Rongved (1955), Plevako (1969), Pan and Chou (1979), Vijayakumar and Cormack (1987b), Yu and Sanday (1991), Hasegawa *et al.* (1992a), as well as Yue (1995). In all these studies, the bi-material interface is assumed to be fully bonded.

In this paper, closed-form Green's functions are presented for a transversely isotropic bi-material solid of infinite extent with a slipping interface. The isotropic planes of the anisotropic bi-material solid are parallel to the slipping interface. Green's functions due to concentrated point and ring force vectors are simultaneously examined using Fourier integral transforms (Fig. 1). In particular, the ring force vector is a force vector uniformly concentrated along a circular ring in the interior of the bi-material solid. The loaded circular ring is parallel to the bi-material interface. The closed-form (Green's functions due to the ring force vector can be utilized in

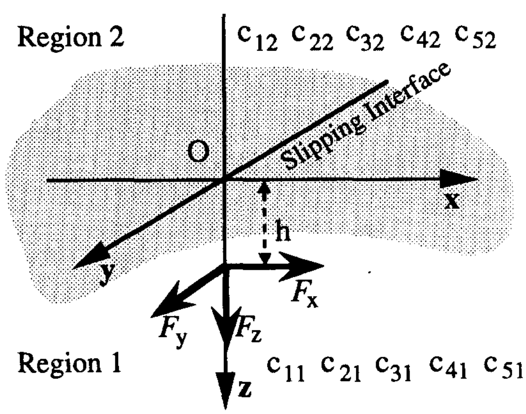

(a) Point force vector (Fx,Fy,Fz)

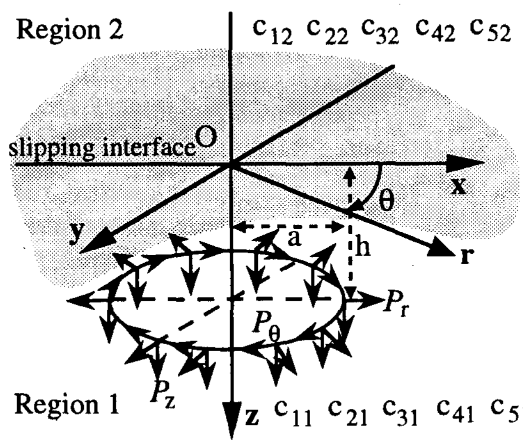

(b) Ring force vector (Pr, Pθ, Pz)

Fig. 1 A transversely isotropic bi-material solid with a slipping interface subjected to force vectors.

eigenstrain and boundary element methods to more effectively solve axisymmetric and torsional boundary value problems in elasticity (Hasegawa and Kondou 1987, Hasegawa *et al.* 1992b). For the concentrated point force vector, the Green functions are expressed in terms of elementary harmonic functions. For the concentrated ring force vector, the Green functions are expressed in terms of the complete elliptic integrals. Numerical results are presented to illustrate the effect of anisotropic bi-material properties on the transmission of normal contact stress and the discontinuity of lateral displacements at the slipping interface. The Green's functions are systematically presented in matrix forms which can be easily implemented in numerical schemes. The closed-form results can also be used as benchmark solutions for the development and verification of purely computational schemes such as finite element methods to attack mechanical problems in bi-solids associated with a Mohr-Coulomb type frictional interface.

2. Boundary conditions and governing equations

We consider the Green's functions of elastic fields in two joined dissimilar transversely isotropic solids subjected to concentrated point and ring body force vectors. The first solid occupies the halfspace region ($k=1$; $0^+ \leq z < +\infty$) and has c_{j1} ($j=1\sim5$) as the five transveresly isotropic material constants. The second solid occupies the halfspace region ($k=2$; $-\infty < z \leq 0^-$) and has c_{j2} ($j=1\sim5$) as the five transveresly isotropic material constants. The two dissimilar solids are bonded without friction at the interface $z=0$, i.e., $u_z|_{z=0^+}=u_z|_{z=0^-}$, $\sigma_{zz}|_{z=0^+}=\sigma_{zz}|_{z=0^-}$, and $\sigma_{xz}|_{z=0^\pm}=\sigma_{yz}|_{z=0^\pm}=0$. For the force vector $\boldsymbol{f}(x, y, z)$ concentrated at a point $(0, 0, h)$ (Fig. 1a), the Cartesian coordinate system $(Oxyz)$ is used and $\boldsymbol{f}(x, y, z)=\boldsymbol{F}_c\delta(x)\delta(y)\delta(z-h)$, where $\delta(\ )$ is a Dirac delta function and $\boldsymbol{F}_c=(F_x, F_y, F_z)^T$. The superscript T stands for the transpose of matrix. For the force vector $\boldsymbol{f}(r, \theta, z)$ concentrated uniformly along a circular ring ($r=a$, $z=h$) (Fig. 1b), the cylindrical coordinate system $(Or\theta z)$ is used and $\boldsymbol{f}(r, \theta, z)=\boldsymbol{P}_a\delta(r-a)\delta(z-h)/(2\pi r)$, where a is the radius of the loaded circle, and $\boldsymbol{P}_a=(P_r, P_\theta, P_z)^T$. Without loss of generality, the body force vectors are assumed to be located in the interior of the first solid ($k=1$), i.e., $h>0$.

A brief account of the governing equations can be presented as follows in a Cartesian tensor notation. The constitutive equations governing the linear relations between stresses (σ_{ij}) and strains (ε_{ij}) in the bi-material transversely isotropic solid take the form

$$
\begin{aligned}
\sigma_{xx}&=c_{1k}\,\varepsilon_{xx}+[c_{1k}-2c_{5k}]\varepsilon_{yy}+c_{2k}\,\varepsilon_{zz}, & \sigma_{xz}&=2c_{4k}\,\varepsilon_{xz}\\
\sigma_{yy}&=[c_{1k}-2c_{5k}]\varepsilon_{xx}+c_{1k}\,\varepsilon_{yy}+c_{2k}\,\varepsilon_{zz}, & \sigma_{yz}&=2c_{4k}\,\varepsilon_{yz}\\
\sigma_{zz}&=c_{2k}\,\varepsilon_{xx}+c_{2k}\,\varepsilon_{yy}+c_{3k}\,\varepsilon_{zz}, & \sigma_{xy}&=2c_{5k}\,\varepsilon_{xy}.
\end{aligned}
\tag{1}
$$

The strains are related to the displacements (u_i) by

$$\varepsilon_{ij}=\frac{1}{2}(u_{i,j}+u_{j,i}). \tag{2}$$

The governing equations are complete with the specification of equations of static equilibrium.

$$\sigma_{ij,j}+f_i=0 \tag{3}$$

where f_i is the body force vector; $i, j=x, y,$ or z; for $z\geq 0^+$, the subscript $k=1$; and for $z\leq 0^-$, the subscript $k=2$.

3. Governing equations in the transform domain

We take the two dimensional (2-D) Fourier integral transforms of Eqs. (1) to (3) with respect to the horizontal coordinates (x, y) in the Cartesian coordinate system (Sneddon 1972). As a result, we obtain the following sets of solution representations for the field variables in a transversely isotropic elastic halfspace (Yue 1995).

$$\boldsymbol{u}(x, y, z)=\frac{1}{2\pi}\int_{-}^{+}\int_{\infty}^{\infty}\frac{1}{\rho}\boldsymbol{\Pi w}(\xi, \eta, z)K\,d\xi d\eta$$

$$\boldsymbol{T}_z(x, y, z)=\frac{1}{2\pi}\int_{-}^{+}\int_{\infty}^{\infty}\boldsymbol{\Pi Y}_z(\xi, \eta, z)K\,d\xi d\eta$$

$$\boldsymbol{\Gamma}_p(x, y, z)=\frac{1}{2\pi}\int_{-}^{+}\int_{\infty}^{\infty}\boldsymbol{\Pi}_p\boldsymbol{w}(\xi, \eta, z)K\,d\xi d\eta$$

$$\boldsymbol{w}(\xi, \eta, z)=\frac{1}{2\pi}\int_{-}^{+}\int_{\infty}^{\infty}\rho\boldsymbol{\Pi}^*\boldsymbol{u}(x, y, z)K^*\,dxdy$$

$$\boldsymbol{Y}_z(\xi, \eta, z)=\frac{1}{2\pi}\int_{-}^{+}\int_{\infty}^{\infty}\boldsymbol{\Pi}^*\boldsymbol{T}_z(x, y, z)\,K^*\,dxdy$$

$$\boldsymbol{g}(\xi, \eta, z)=\frac{1}{2\pi}\int_{-}^{+}\int_{\infty}^{\infty}\boldsymbol{\Pi}^*\boldsymbol{f}(x, y, z)K^*\,dxdy \tag{4}$$

where $K=e^{i(\xi x+\eta y)}$ and $i=\sqrt{-1}$. The above 2-D integrals are in the sense of the Cauchy principal values. The vector fields in Eqs. (4) are defined by $\boldsymbol{u}=[u_x, u_y, u_z]^T$, $\boldsymbol{T}_z=[\sigma_{xz}, \sigma_{yz}, \sigma_{zz}]^T$, $\boldsymbol{f}=[f_x, f_y, f_z]^T$, $\boldsymbol{\Gamma}_p=[\varepsilon_{xx}, \varepsilon_{xy}, \varepsilon_{yy}]^T$, $\boldsymbol{w}=[w_1, w_2, w_3]^T$, $\boldsymbol{Y}_z=[\tau_1, \tau_2, \tau_3]^T$, and $\boldsymbol{g}=[g_1, g_2, g_3]^T$. $\boldsymbol{K}^*$ and $\boldsymbol{\Pi}^*$ are respectively the complex conjugates of $\boldsymbol{K}$ and $\boldsymbol{\Pi}$.

$$\boldsymbol{\Pi}=\begin{pmatrix}\frac{i\xi}{\rho} & \frac{i\eta}{\rho} & 0\\ \frac{i\eta}{\rho} & \frac{-i\xi}{\rho} & 0\\ 0 & 0 & 1\end{pmatrix},\quad \boldsymbol{\Pi}_p=-\begin{pmatrix}\frac{\xi^2}{\rho^2} & \frac{\xi\eta}{\rho^2} & 0\\ \frac{\xi\eta}{\rho^2} & \frac{\eta^2-\xi^2}{\rho^2} & 0\\ \frac{\eta^2}{\rho^2} & \frac{\xi\eta}{\rho^2} & 0\end{pmatrix} \tag{5}$$

In the following, we shall note that $\boldsymbol{w}(z)=\boldsymbol{w}(\xi, \eta, z)$, $\boldsymbol{Y}_z(z)=\boldsymbol{Y}_z(\xi, \eta, z)$ $\boldsymbol{g}(z)=\boldsymbol{g}(\xi, \eta, z)$ for simplicity. In particular, $\boldsymbol{g}(z)=\boldsymbol{g}\delta(z-h)$ for the body force vectors concentrated at the horizontal plane $z=h$.

The partial differential Eqs. (1)~(3) governing the behaviour of a transversely isotropic solid can then be reduced to two sets of first-order ordinary differential equations in the Fourier transform domain. Solving these ordinary differential equations, we can obtain algebraic equations governing the field variables in the bi-materials transversely isotropic solid.

(i) For $k=1(0^+ \leq z < +\infty)$, the algebraic governing equations can be expressed as follows in terms of the six boundary variables at $z=0^+$.

$$
\begin{aligned}
2\boldsymbol{w}(z) &= \left[\sum_{n=0}^{2} e^{-\rho z\gamma_{n1}} \boldsymbol{A}_{n1}\right]\boldsymbol{w}(0^+) + \left[\sum_{n=0}^{2} e^{-\rho z\gamma_{n1}} \boldsymbol{B}_{n1}\right]\boldsymbol{Y}_z(0^+) + \left[\sum_{n=0}^{2} e^{-\rho|z-h|\gamma_{n1}} \boldsymbol{\Phi}_n\right]\boldsymbol{g} \\
2\boldsymbol{Y}_z(z) &= \left[\sum_{n=0}^{2} e^{-\rho z\gamma_{n1}} \boldsymbol{C}_{n1}\right]\boldsymbol{w}(0^+) + \left[\sum_{n=0}^{2} e^{-\rho z\gamma_{n1}} \boldsymbol{D}_{n1}\right]\boldsymbol{Y}_z(0^+) + \left[\sum_{n=0}^{2} e^{-\rho|z-h|\gamma_{n1}} \boldsymbol{\Psi}_n\right]\boldsymbol{g}.
\end{aligned}
\tag{6}
$$

(ii) For $k=2(-\infty < \gamma_{n1} z \leq 0^-)$, the algebraic governing equations can be expressed as follows in terms of the six boundary variables at $z=0^-$.

$$
\begin{aligned}
2\boldsymbol{w}(z) &= \left[\sum_{n=0}^{2} e^{\rho z\gamma_{n2}} \boldsymbol{A}_{n2}\right]\boldsymbol{w}(0^-) + \left[\sum_{n=0}^{2} e^{\rho z\gamma_{n2}} \boldsymbol{B}_{n2}\right]\boldsymbol{Y}_z(0^-) \\
2\boldsymbol{Y}_z(z) &= \left[\sum_{n=0}^{2} e^{\rho z\gamma_{n2}} \boldsymbol{C}_{n2}\right]\boldsymbol{w}(0^-) + \left[\sum_{n=0}^{2} e^{\rho z\gamma_{n2}} \boldsymbol{D}_{n2}\right]\boldsymbol{Y}_z(0^-)
\end{aligned}
\tag{7}
$$

where $\boldsymbol{A}_{nk}$, $\boldsymbol{B}_{nk}$, $\boldsymbol{C}_{nk}$, $\boldsymbol{D}_{nk}$, $\boldsymbol{\Phi}_n$, and $\boldsymbol{\Psi}_n$ $(n=0, 1, 2;\ k=1, 2)$ are 30 constant square matrices and are given exactly in Appendix A. $\gamma_{0k}=\sqrt{\dfrac{c_5 k}{c_4 k}}$; $\gamma_{1k}=\alpha_k+\beta_k$, $\gamma_{2k}=\alpha_k-\beta_k$, where

$$
\alpha_k=\left[\frac{(\sqrt{c_{1k}c_{3k}}-c_{2k})(\sqrt{c_{1k}c_{3k}}+c_{2k}+2c_{4k})}{4c_{3k}c_{4k}}\right]^{1/2} \text{ and } \beta_k=\left[\frac{(\sqrt{c_{1k}c_{3k}}+c_{2k})(\sqrt{c_{1k}c_{3k}}-c_{2k}-2c_{4k})}{4c_{3k}c_{4k}}\right]^{1/2}.
$$

If $\sqrt{c_{1k}c_{3k}}-c_{2k}-2c_{4k}=0$, (then $\gamma_{1k}=\gamma_{2k}=(c_{1k}/c_{3k})^{1/4}$), the governing equations for $\boldsymbol{w}(z)$ and $\boldsymbol{Y}_z(z)$ can be obtained by taking the limit as $\gamma_{1k}\rightarrow\gamma_{2k}$ in Eqs. (6) and (7). This degenerated case includes the solids which exhibit isotropic material properties, where $\gamma_{0k}=\gamma_{1k}=\gamma_{2k}=1$, $c_{1k}=c_{3k}=\lambda_k+2\mu_k$, $c_{2k}=\lambda_k$, and $c_{4k}=c_{5k}=\mu_k$; λ_k and μ_k are the Lame's constants.

4. Green's functions in the transform domain

By putting $z=0^+$ into Eq. (6) and $z=0^-$ into Eq. (7), we can have six independent algebraic equations governing the twelve unknown boundary variables $\boldsymbol{w}(0^\pm)$ and $\boldsymbol{Y}_z(0^\pm)$ at the slipping interface. Using the slipping interface condition, we can have the following six results of $\boldsymbol{w}(0^\pm)$ and $\boldsymbol{Y}_z(0^\pm)$: $w_3(0^+)=w_3(0^-)$, $\tau_3(0^+)=\tau_3(0^-)$, $\tau_1(0^+)=\tau_1(0^-)=0$, and $\tau_2(0^+)=\tau_2(0^-)=0$. Solving the twelve independent linear algebraic equations, we can obtain the following solution for $w(0^\pm)$ and $\boldsymbol{Y}_z(0^\pm)$ in terms of $\boldsymbol{g}$.

$$
\begin{aligned}
\boldsymbol{w}(0^+) &= \left[\sum_{n=0}^{2} e^{-\rho h\gamma_{n1}} \boldsymbol{P}_{n1}\right]\boldsymbol{g} \\
\boldsymbol{w}(0^-) &= \left[\sum_{n=0}^{2} e^{-\rho h\gamma_{n1}} \boldsymbol{P}_{n2}\right]\boldsymbol{g} \\
\boldsymbol{Y}_z(0^+) = \boldsymbol{Y}_z(0^-) &= \left[\sum_{n=0}^{2} e^{-\rho h\gamma_{n1}} \boldsymbol{Q}_n\right]\boldsymbol{g}
\end{aligned}
\tag{8}
$$

where $\boldsymbol{P}_{nk}$ ($k=1$, $n=0$, 1, 2; $k=2$, $n=1$, 2) and $\boldsymbol{Q}_n$ ($n=1$, 2) are 7 constant square matrices and are given exactly in Appendix A.

Substituting the results of Eq. (4) into Eqs. (6) and (7), we can obtain the Green's functions of $\boldsymbol{w}(z)$ and $\boldsymbol{Y}_z(z)$ in terms of $\boldsymbol{g}$ as follows.

(i) In the solid region $k=(0^+ \leq z < +\infty)$, we have

$$2\boldsymbol{w}(z)=\left[\sum_{m=0}^{4} e^{-\rho z_{m1}} \boldsymbol{\Phi}_{m1}+\sum_{n=0}^{2} e^{-\rho|z-h|\gamma_{n1}} \boldsymbol{\Phi}_n\right]\boldsymbol{g}$$

$$2\boldsymbol{Y}_z(z)=\left[\sum_{m=0}^{4} e^{-\rho z_{m1}} \boldsymbol{\Psi}_{m1}+\sum_{n=0}^{2} e^{-\rho|z-h|\gamma_{n1}} \boldsymbol{\Psi}_n\right]\boldsymbol{g} \tag{9}$$

(ii) In the solid region $k=2(-\infty < z \leq 0^-)$, we have

$$2\boldsymbol{w}(z)=\left[\sum_{m=0}^{4} e^{-\rho z_{m2}} \boldsymbol{\Phi}_{m2}\right]\boldsymbol{g}$$

$$2\boldsymbol{Y}_z(z)=\left[\sum_{m=0}^{4} e^{-\rho z_{m2}} \boldsymbol{\Psi}_{m2}\right]\boldsymbol{g} \tag{10}$$

where $z_{01}=\gamma_{01}(h+z)$, $z_{11}=\gamma_{11}(h+z)$, $z_{21}=\gamma_{11}h+\gamma_{21}z$, $z_{31}=\gamma_{21}h+\gamma_{11}z$, $z_{41}=\gamma_{21}(h+z)$; $z_{12}=\gamma_{11}h-\gamma_{12}z$, $z_{22}=\gamma_{11}h-\gamma_{22}z$, $z_{32}=\gamma_{21}h-\gamma_{12}z$, $z_{42}=\gamma_{21}h-\gamma_{22}z$; and $\boldsymbol{\Phi}_{mk}$ and $\boldsymbol{\Psi}_{mk}$ ($k=1$, $m=0$, 1, 2, 3, 4; $k=2$, $m=1$, 2, 3, 4) are 18 constant square matrices and given exactly as follows:

$$\begin{aligned}
\boldsymbol{\Phi}_{01}&=\boldsymbol{A}_{01}\boldsymbol{P}_{01}\\
\boldsymbol{\Psi}_{01}&=\boldsymbol{C}_{01}\boldsymbol{P}_{01}\\
\boldsymbol{\Phi}_{1k}&=\boldsymbol{A}_{1k}\boldsymbol{P}_{1k}+\boldsymbol{B}_{1k}\boldsymbol{Q}_1\\
\boldsymbol{\Phi}_{2k}&=\boldsymbol{A}_{2k}\boldsymbol{P}_{1k}+\boldsymbol{B}_{2k}\boldsymbol{Q}_1\\
\boldsymbol{\Phi}_{3k}&=\boldsymbol{A}_{1k}\boldsymbol{P}_{2k}+\boldsymbol{B}_{1k}\boldsymbol{Q}_2\\
\boldsymbol{\Phi}_{4k}&=\boldsymbol{A}_{2k}\boldsymbol{P}_{2k}+\boldsymbol{B}_{2k}\boldsymbol{Q}_2\\
\boldsymbol{\Psi}_{1k}&=\boldsymbol{C}_{1k}\boldsymbol{P}_{1k}+\boldsymbol{D}_{1k}\boldsymbol{Q}_1\\
\boldsymbol{\Psi}_{2k}&=\boldsymbol{C}_{2k}\boldsymbol{P}_{1k}+\boldsymbol{D}_{2k}\boldsymbol{Q}_1\\
\boldsymbol{\Psi}_{3k}&=\boldsymbol{C}_{1k}\boldsymbol{P}_{2k}+\boldsymbol{D}_{1k}\boldsymbol{Q}_2\\
\boldsymbol{\Psi}_{4k}&=\boldsymbol{C}_{2k}\boldsymbol{P}_{2k}+\boldsymbol{D}_{2k}\boldsymbol{Q}_2
\end{aligned}$$

5. Green's functions in the physical domain

5.1. A general force vector

For simplicity, we re-express the solution of $\boldsymbol{w}(z)$ and $\boldsymbol{Y}_z(z)$ in Eqs. (9) and (10) in the following general form.

$$\boldsymbol{w}(z)=\boldsymbol{\Phi}\boldsymbol{g}, \qquad \boldsymbol{Y}_z(z)=\boldsymbol{\Psi}\boldsymbol{g} \tag{11}$$

where $\boldsymbol{\Phi}$ and $\boldsymbol{\Psi}$ are square matrices and are functions of ρz and ρh. Using Eqs. (4) and (11), we can systematically present the solution of the displacements $\boldsymbol{u}$, the vertical stresses $\boldsymbol{T}_z$, and the plane strains $\boldsymbol{\Gamma}_p$ in the bi-material solid due to a general body force vector $\boldsymbol{f}(x, y)\,\delta(z-h)$ concentrated at the horizontal plane $z=h$.

$$u=\frac{1}{2\pi}\int_{-}^{+}\int_{\infty}^{\infty}\frac{1}{\rho}\Pi\Phi g K\,d\xi d\eta$$

$$T_z=\frac{1}{2\pi}\int_{-}^{+}\int_{\infty}^{\infty}\Pi\Psi g K\,d\xi d\eta$$

$$\Gamma_p=\frac{1}{2\pi}\int_{-}^{+}\int_{\infty}^{\infty}\Pi_p\Phi g K\,d\xi d\eta \quad (12)$$

where $-\infty<x,\ y,\ z<+\infty$.

5.2. The point force vector

For the concentrated point force vector, we have $g=\Pi^*F_c/(2\pi)$. The solution can then be expressed in the forms of 2-D inverse Fourier transforms.

$$u=\frac{1}{4\pi^2}\int_{-}^{+}\int_{\infty}^{\infty}\frac{1}{\rho}\Pi\Phi\Pi^* g K\,d\xi d\eta F_c$$

$$T_z=\frac{1}{4\pi^2}\int_{-}^{+}\int_{\infty}^{\infty}\Pi\Psi\Pi^* g K\,d\xi d\eta F_c$$

$$\Gamma_p=\frac{1}{4\pi^2}\int_{-}^{+}\int_{\infty}^{\infty}\Pi_p\Phi\Pi^* g K\,d\xi d\eta F_c \quad (13)$$

where $-\infty<x,\ y,\ z<+\infty,\ \sqrt{x^2+y^2+(z-h)^2}\neq 0$.

5.3. The ring force vector

In the ensuing, the cylindrical coordinates systems are used for Green's functions due to the force vector uniformly concentrated along a circular ring ($r=a,\ z=h$). The relationships between the Cartesian and cylindrical coordinate systems in both physical and transform domains are defined by $x=r\cos\theta,\ y=r\sin\theta$; and $\xi=\rho\sin\varphi,\ \eta=\rho\cos\varphi$. After the coordinate transformation, the solution in Eq. (12) can be expressd in the forms of Fourier series expansions. In particular, for the concentrated ring force vector, the solution can be expressed in the forms of Hankel transform integral involving the products of the Bessel functions of order zero to second.

$$u=\int_0^{\infty}\Pi_0(\rho r)\,\Phi\Pi_0(\rho a)d\rho\,P_a$$

$$T_z=\int_0^{\infty}\rho\Pi_0(\rho r)\,\Psi\Pi_0(\rho a)d\rho\,P_a$$

$$\Gamma_p=\int_0^{\infty}\rho\Pi_{p0}(\rho r)\,\Phi\Pi_0(\rho a)d\rho\,P_a \quad (14)$$

where $0 \leq r < +\infty$, $0 \leq \theta < 2\pi$, $-\infty < z < +\infty$ and $\sqrt{(r-a)^2+(z-h)^2} \neq 0$; $u=[u_r, u_\theta, u_z]^T$; $T_z=[\sigma_{rz}, \sigma_{\theta z}, \sigma_{zz}]^T$; $\Gamma_p=[\varepsilon_{\theta\theta}, \varepsilon_{\theta r}, \varepsilon_{rr}]^T$. The matrices $\Pi_0(\chi)$ and $\Pi_{p0}(\chi)$ are defined by

$$\Pi_0(\chi)=\begin{pmatrix} -J_1(\chi) & 0 & 0 \\ 0 & J_1(\chi) & 0 \\ 0 & 0 & J_0(\chi) \end{pmatrix}$$

$$\Pi_{p0}(\chi)=-\frac{1}{2}\begin{pmatrix} J_0(\chi)-J_2(\chi) & 0 & 0 \\ 0 & J_2(\chi) & 0 \\ J_0(\chi)+J_2(\chi) & 0 & 0 \end{pmatrix} \tag{15}$$

where $J_m(\chi)$ is the Bessel functions of order $m(m=0, 1, 2)$.

5.4. Closed-form Green's functions

The improper integral in Eqs. (13) and (14) can be analytically calculated. As a result, closed-form solutions can be obtained for the Green's functions associated with the concentrated point and ring force vectors as follows.

(i) In the solid $k=1(z \leq 0^+)$, we have

$$\begin{aligned} \boldsymbol{u} &= \left[\sum_{m=0}^{4} \boldsymbol{G}_v[0, z_{m1}, \boldsymbol{\Phi}_{m1}] + \sum_{n=0}^{2} \boldsymbol{G}_v[0, |z-h|\gamma_{n1}, \boldsymbol{\Phi}_n]\right]\boldsymbol{F} \\ \boldsymbol{T}_z &= \left[\sum_{m=0}^{4} \boldsymbol{G}_v[0, z_{m1}, \boldsymbol{\Psi}_{m1}] + \sum_{n=0}^{2} \boldsymbol{G}_v[1, |z-h|\gamma_{n1}, \boldsymbol{\Psi}_n]\right]\boldsymbol{F} \\ \boldsymbol{\Gamma}_p &= \left[\sum_{m=0}^{4} \boldsymbol{G}_p[0, z_{m1}, \boldsymbol{\Phi}_{m1}] + \sum_{n=0}^{2} \boldsymbol{G}_p[1, |z-h|\gamma_{n1}, \boldsymbol{\Phi}_n]\right]\boldsymbol{F} \end{aligned} \tag{16}$$

(ii) In the solid $k=2(z \leq 0^-)$, we have

$$\begin{aligned} \boldsymbol{u} &= \left[\sum_{m=1}^{4} \boldsymbol{G}_v[0, z_{m2}, \boldsymbol{\Phi}_{m2}]\right]\boldsymbol{F} \\ \boldsymbol{T}_z &= \left[\sum_{m=1}^{4} \boldsymbol{G}_v[1, z_{m2}, \boldsymbol{\Psi}_{m2}]\right]\boldsymbol{F} \\ \boldsymbol{\Gamma}_p &= \left[\sum_{m=1}^{4} \boldsymbol{G}_p[1, z_{m2}, \boldsymbol{\Phi}_{m2}]\right]\boldsymbol{F} \end{aligned} \tag{17}$$

a) For the point force vector, the solution is presented in the Cartesian coordinate system $(Oxyz)$ $\boldsymbol{F}=\boldsymbol{F}_c$. The square matrices $\boldsymbol{G}_v[\alpha, z, \boldsymbol{\Phi}]$ and $\boldsymbol{G}_p[\alpha, z, \boldsymbol{\Phi}]$ ($\alpha=0, 1$; $z \geq 0$) are defined in the following

$$4\pi G_v[\alpha, z, \boldsymbol{S}]=\frac{1}{2\pi}\int_{-}^{+}\int_{\infty}^{\infty} \rho^{\alpha-1}e^{-\rho z}\, \boldsymbol{\Pi} \boldsymbol{S}\, \boldsymbol{\Pi}^* K\, d\xi d\eta$$

$$=S_{22}\begin{pmatrix} g_{\alpha 02}(z) & -g_{\alpha 11}(z) & 0 \\ -g_{\alpha 11}(z) & g_{\alpha 20}(z) & 0 \\ 0 & 0 & 0 \end{pmatrix}$$

$$+\begin{pmatrix} S_{11}g_{\alpha20}(z) & S_{11}g_{\alpha11}(z) & S_{13}g_{\alpha10}(z) \\ S_{11}g_{\alpha11}(z) & S_{11}g_{\alpha02}(z) & S_{13}g_{\alpha01}(z) \\ -S_{31}g_{\alpha10}(z) & -S_{31}g_{\alpha01}(z) & S_{33}g_{\alpha00}(z) \end{pmatrix}$$

$$4\pi G_p[\alpha,\ z,\ \boldsymbol{S}]=\frac{1}{2\pi}\int_{-}^{+}\int_{\infty}^{\infty}\ \rho^{\alpha-1}e^{-\rho z}\Pi p S \Pi^* K\, d\xi d\eta$$

$$=S_{22}\begin{pmatrix} g_{\alpha12}(z) & -g_{\alpha21}(z) & 0 \\ \frac{1}{2}[g_{\alpha03}(z)-g_{\alpha21}(z)] & \frac{1}{2}[g_{\alpha30}(z)-g_{\alpha12}(z)] & 0 \\ -g_{\alpha12}(z) & g_{\alpha21}(z) & 0 \end{pmatrix}$$

$$+\begin{pmatrix} S_{11}g_{\alpha30}(z) & S_{11}g_{\alpha21}(z) & -S_{13}g_{\alpha20}(z) \\ S_{11}g_{\alpha21}(z) & S_{11}g_{\alpha12}(z) & -S_{13}g_{\alpha11}(z) \\ -S_{11}g_{\alpha12}(z) & S_{11}g_{\alpha03}(z) & -S_{13}g_{\alpha02}(z) \end{pmatrix} \tag{18}$$

where $g_{\alpha ij}(z)$ $(0\leq i+j\leq 3)$ are elementary functions and are given explicitly in Appendix B.

b) For the ring force vector, the solution is presented in the cylindrical coordinate system $(O r\theta z)$, $\boldsymbol{F}=\boldsymbol{P}_a$. The square matrices $\boldsymbol{G}_v[\alpha,\ z,\ \boldsymbol{\Phi}]$ and $\boldsymbol{G}_p[\alpha,\ z,\ \boldsymbol{\Phi}]$ $(\alpha=0,\ 1;\ z\geq 0)$ are defined in the following.

$$4\pi G_v[\alpha,\ z,\ S]=\int_0^{\infty}\rho^{\alpha}e^{-\rho z}\Pi_0(\rho r) S\, \Pi_0(\rho a)d\rho$$

$$=\begin{pmatrix} S_{11}q_{\alpha11}(z) & 0 & -S_{13}q_{\alpha10}(z) \\ 0 & S_{22}q_{\alpha11}(z) & 0 \\ -S_{31}q_{\alpha01}(z) & 0 & S_{33}q_{\alpha00}(z) \end{pmatrix}$$

$$4\pi G_p[\alpha+1,\ z,\ S]=\int_0^{\infty}\rho^{\alpha}e^{-\rho z}\Pi_{p0}(\rho r) S\, \Pi_0(\rho \alpha)d\rho$$

$$=\begin{pmatrix} S_{11}q_{(\alpha+1)01}(z) & 0 & -S_{13}q_{(\alpha+1)00}(z) \\ 0 & \frac{1}{2}S_{22}q_{(\alpha+1)01}(z) & 0 \\ 0 & 0 & 0 \end{pmatrix}$$

$$-\frac{1}{r}\begin{pmatrix} S_{11}q_{\alpha11}(z) & 0 & -S_{13}q_{\alpha10}(z) \\ 0 & S_{22}q_{\alpha11}(z) & 0 \\ -S_{11}q_{\alpha11}(z) & 0 & S_{13}q_{\alpha10}(z) \end{pmatrix} \tag{19}$$

where $q_{\alpha ij}(z)$ $(i=0,\ 1;\ j=0,\ 1)$ are functions of the complete elliptic integrals and are given explicitly in Appendix B. In Eqs. (18) and (19), $\boldsymbol{S}$ is a constant square matrix and is defined by

$$S=\begin{pmatrix} S_{11} & 0 & S_{13} \\ 0 & S_{22} & 0 \\ S_{31} & 0 & S_{33} \end{pmatrix} \tag{20}$$

The solution of the vertical strains $\boldsymbol{\Gamma}_z=[\varepsilon_{13},\ \varepsilon_{23},\ \varepsilon_{33}]^T$ and the plane stresses $\boldsymbol{T}_p=[\sigma_{11},\ \sigma_{12},\ \sigma_{22}]^T$

can be easily and uniquely found by using the constitutive relation Eq. (1) and the solution of $\boldsymbol{\Gamma}_p$ and $\boldsymbol{T}_z$.

6. Numerical results

Two transversely isotropic materials are selected for the numerical evaluation. One is magnesium (c_1=41.19, c_2=14.79, c_3=42.57, c_4=11.32, c_5=11.56 kPa) and the other is zinc (c_1=111.02, c_2=34.57, c_3=42.09, c_4=26.43, c_5=43.95 kPa) (Lin and Keer 1989). Two isotropic solids called m-iso (λ=19.0, μ=11.44 kPa) and z-iso (λ=6.175, μ=35.19 kPa) may be estimated from magnesium and zinc, respectively, using the assumption that $\mu=0.5(c_4+c_5)$ and $\lambda+2\mu=0.5(c_1+c_3)$. As a result, we have the following four cases of material properties for the bi-materials:

case 1: magnesium for $z\geq0^+$ and magnesium for $z\leq0^-$;
case 2: magnesium for $z\geq0^+$ and zinc for $z\leq0^-$;
case 3: m-iso for $z\geq0^+$ and z-iso for $z\leq0^-$ and;
case 4: m-iso for $z\geq0^+$ and m-iso for $z\leq0^-$.

In particular, case 1 (or case 4) represent a transversely isotropic (or an isotropic) elastic solid of infinite extent with a slipping interface.

Fig. 2 and Fig. 3 illustrate the transmission of normal contact stresses at the slipping interface due to the point forces (F_x, F_z) and the ring forces (P_r, P_z), respectively. The normal contact stress distribution are different for the four cases of the bi-material properties. The normal contact stress may be tensile if an inclined point (or ring) force acting toward the slipping interface, which means the slipping interface must be precompressed (Dundurs and Hetenyi, 1965).

Fig. 4 and Fig. 5 illustrate the discontinuities of lateral displacements at the slipping interface of the bi-material case 2 due to the point forces (F_x, F_z) and ring forces (P_r, P_θ, P_z), respectively. The corresponding displacements at a fully bonded (rough) interface of the bi-material are continuous and also plotted in Fig. 4 and Fig. 5 for comparison purpose (Yue 1995). The absolute values of the lateral displacements at $z=0^+$ the slipping interface are always greater than those

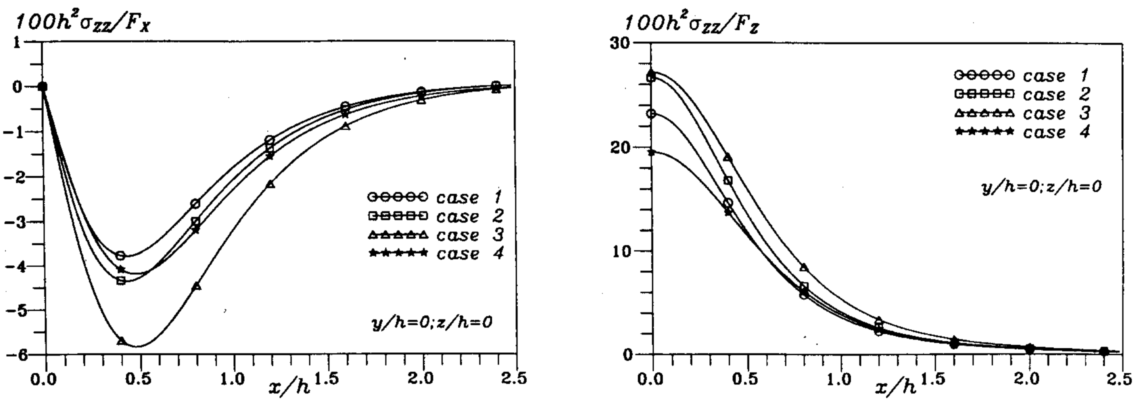

(a) (b)

Fig. 2 Transmission of normal contact stress between the slipping bi-material interface due to point forces (F_x, F_z).

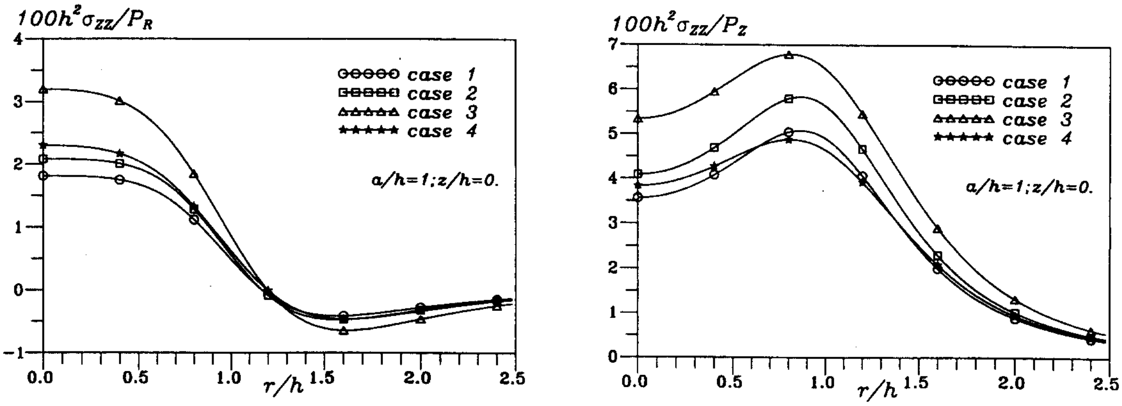

(a) (b)

Fig. 3 Transmission of normal contact stress between the slipping bi-material interface due to ring forces (P_R, P_z).

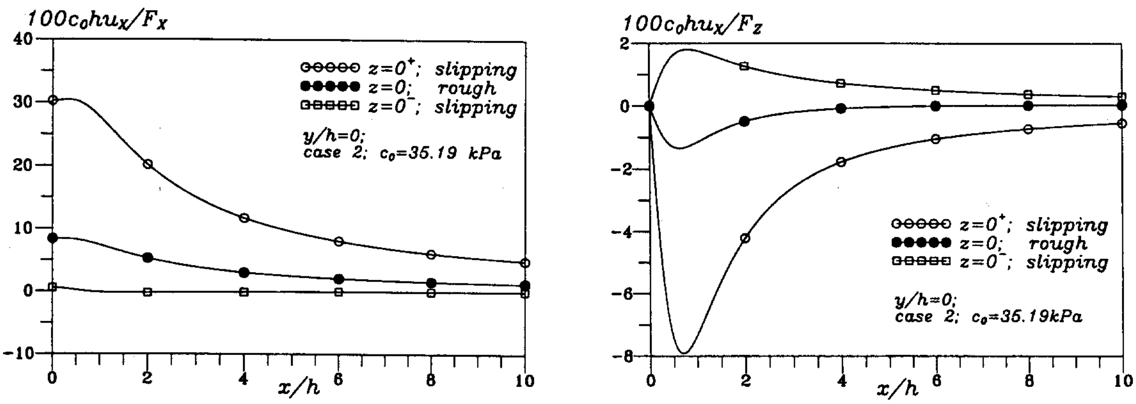

(a) (b)

Fig. 4 Discontinuities of lateral displacements at the slipping bi-material interface due to point forces (F_x, F_z).

of the corresponding displacements at the rough interface. The lateral displacements at $z=0^+$ of the slipping interface always have the same directions as the corresponding displacements at the rough interface. But, the lateral displacements at $z=0^\pm$ of the slipping interface can have opposite directions. The torsional ring force P_θ acting in the bi-material region $k=1$ does not generate any deformation in the bi-material region $k=2$ if the interface is slipping.

7. Concluding remarks

(1) By using the classical Fourier transform technique, closed-form Green's functions are obtained for the elastic fields in a transversely isotropic bi-material solid with a slipping interface subjected to concentrated point and ring force vectors.
(2) As special cases, closed-form Green's functions are also obtained for problems of (i) a

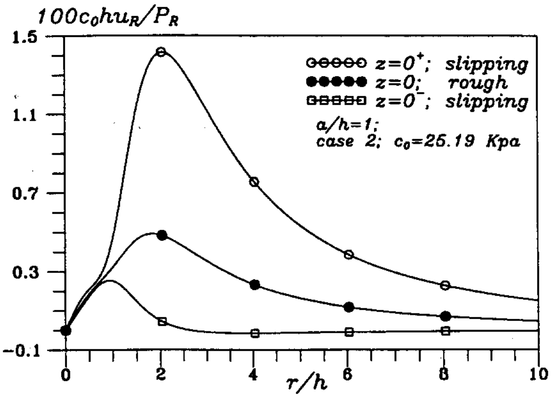

(a)

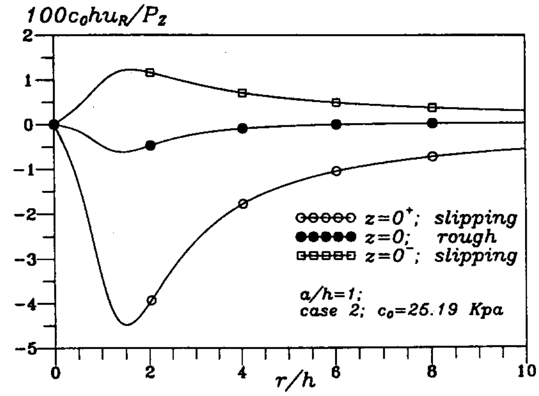

(b)

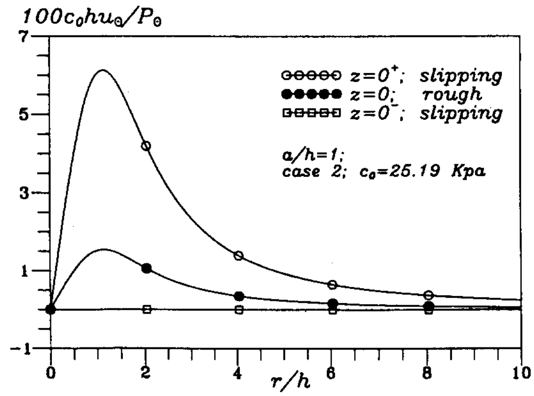

(c)

Fig. 5 Discontinuities of lateral displacements at the slipping bi-material interface due to ring forces (P_R, P_θ, P_z).

transversely isotropic elastic halfspace smoothly joined with an isotropic elastic halfspace; (ii) two isotropic elastic halfspace with a slipping interface; (iii) a transversely isotropic (or an isotropic) elastic infinite space; and (iv) a transversely isotropic (or an isotropic) elastic halfspace with either a traction-free boundary or a horizontally traction-free and vertically fixed boundary, subjected to the concentrated point and ring force vectors.

(3) The solution presented in Eq. (12) can be further used to examine Green's functions due to other concentrated force vectors such as the force vectors either concentrated along an elliptic (or rectangular) ring or distributed over a circular (or rectangular) area.

(4) The Green's functions are systematically presented in matrix forms which can be easily implemented in numerical schemes such a boundary element methods. The closed-form results can also be used as benchmark solutions for the development and verification of further solutions in bi-solids associated with a Mohr-Coulomb type frictional interface.

References

Dundurs, J. and Hetenyi, H. (1965), "Transmission of force between semi-infinite solids", *Journal of*

Applied Mechanics, ASME, **32**, 671-674.
Dundurs, J. and Stippes, M. (1970), "Role of elastic constants in certain contact problems", *J. of Applied Mechanics, ASME*, **37**, 965-970.
Elliott, H. A. (1948), "Three-dimensional stress distributions in hexagonal aeolotropic crystals", *Proceedings, Cambridge Philosophical Society,* **44**, 522-533.
Eason, G., Noble, B., and Sneddon, I.N. (1955), "On certain integrals of Lipschitz-Hankel type involving products of Bessel functions", *Philosophical Transaction Royal Society,* London, **A247**, 529-551.
Gharpuray, V.M., Dundurs, J. and Keer, L.M. (1991), "A crack terminating at a slipping interface between two materials". *Journal of Applied Mechanics, ASME,* **58**, 960-963.
Gladwell, G.M.L. and Hera, T. (1981), "The contact problem for a rigid obstacle pressed between two dissimilar elastic half-spaces", *Q. Jl Mech. Appl. Math.*, **47**(Pt. 2), 251-263.
Hanson, M.T. (1992), "The elastic field for conical indentation including sliding friction for transverse isotropy", *J. of Applied Mechanics, ASME,* **59**, S123-S130.
Hasegawa, H. and Kondou, K. (1987), "Stress analysis of an elastic half-spae having an axisymmetric cavity." *Theoretical and Applied Mechanics, Proceedings of the 32nd Japan National Congress for Applied Mechanics,* **37**, 339-345.
Hasegawa, H., Lee, V.G. and Mura, T. (1992a), "Green's functions for axisymmetric problems of dissimilar elastic solids", *Journal of Applied Mechanics, ASME,* **59**, 312-320.
Hasegawa, H., Lee, V.G. and Mura, T. (1992b), "The stress fields caused by a circular cylindrical inclusion", *Journal of Applied Mechanics, ASME,* **59**, S107-S114.
Lin, W. and Keer, L.M. (1989), "Three-dimensional analysis of cracks in layered transversely isotropic media", *Proc. R. Soc. Lond. A* **424**, 307-322.
Mura T. 1982, *Micromechanics of Defects in Solids.* Martinus Nijhoff Publishers, Boston.
Pan, Y.C. and Chou, T.W. (1979), "Green's functions for two-phase transversely isotropic materials", *Journal of Applied Mechanics, ASME,* **46**, 551-556.
Plevako, K.P. (1969), "A point force inside a pair of cohering halfspace", *Osnovaniya Fundamental i Mekhanika Gruntov,* No. 3, 9-11.
Rongved, L. (1955), "Force interior to one or two joined semi-infinite solids", *Proc. Sec. Midwest. Conf. Solid Mech.,* Lafayette, Indiana, Prudue University, 1-13.
Selvadurai, A.P.S. (1994), "A unilateral contact problem for a rigid disc inclusion embedded between two dissimilar elastic half-spaces", *Q. Jl Mech. Appl. Math.,* **47**(Pt. 3), 493-510.
Sneddon, I.N. (1972), *The Use of Integral Transform,* McGraw-Hill, New York.
Vijayakumar, S. and Cormack, D.E. (1987a), "Nuclei of strain for bi-material elastic media with sliding interface", *J. Elasticity,* **17**, 285-290.
Vijayakumar, S. and Cormack, D.E. (1987b), "Green's functions for the biharmonic equation: bonded elastic media", *SIAM J. of Applied Mathematics,* **47**, 982-997.
Wijeyewickrema, A.C. and Keer, L.M. (1994), "Axial decay of stresses in a layered composite with slipping interfaces". *Composite Engineering,* **4**(9), 895-899.
Yu, H.Y. and Sanday, S.C. (1991), "Elastic fields in joined half-space due to nuclei of strain", *Proc. R. Soc. Lond.,* **A434**, 503-519.
Yue, Z.Q. (1995), "Elastic fields in two joined transversely isotropic solids due to concentrated forces", *Int. J. Engng. Sci.* **33**(3), 351-369.
Yuuki, R., Cho, S.-B., Matsumoto, T., Kisu, H., (1987), "Efficient boundary element elastostatic analysis using Hetenyi's fundamental solution", *Transaction of Japan Society of Mechanical Engineers,* Series A, **53**, 1581-1589.

Appendix A

The 30 constant square matrices in Eqs. (6) and (7) are given exactly as follows: $A_{01}=A_{02}=D_{01}=D_{02} = \Theta_0$; $B_{01}=\frac{-1}{c_{41}\gamma_{01}}\Theta_0$; $B_{02}=\frac{1}{c_{42}\gamma_{02}}\Theta_0$; $C_{01}=-c_{41}\gamma_{01}\Theta_0$; $C_{02}=c_{42}(\gamma_{02})\Theta_0$; $A_{11}=-\Theta_2(\gamma_{11})$, $A_{12}=-\Theta_2(-\gamma_{12})$,

$A_{21}=\Theta_2(\gamma_{21})$, $A_{22}=\Theta_2(-\gamma_{22})$; $B_{11}=-\Theta_1(\gamma_{11})$, $B_{12}=-\Theta_1(-\gamma_{12})$, $B_{21}=\Theta_1(\gamma_{21})$, $B_{22}=\Theta_1(-\gamma_{22})$; $C_{11}=-\Theta_4(\gamma_{11})$, $C_{12}=-\Theta_4(-\gamma_{21})$, $C_{21}=\Theta_4(\gamma_{21})$, $C_{22}=\Theta_4(-\gamma_{22})$; $D_{11}=-\Theta_3(\gamma_{11})$, $D_{12}=-\Theta_3(-\gamma_{12})$, $D_{21}=\Theta_3(\gamma_{21})$, $D_{22}=\Theta_3(-\gamma_{22})$; $\Phi_0=\frac{1}{c_{41}\gamma_{01}}\Theta_0$, $\Phi_1=\mathrm{SIGN}\ \Theta_1(\mathrm{SIGN}\ \gamma_{11})$, $\Phi_2=-\mathrm{SIGN}\ \Theta_1(\mathrm{SIGN}\ \gamma_{21})$; $\Psi_0=-\mathrm{SIGN}\ \Theta_0$, $\Psi_1=\mathrm{SIGN}\ \Theta_3(\mathrm{SIGN}\ \gamma_{11})$, $\Psi_2=-\mathrm{SIGN}\ \Theta_3(\mathrm{SIGN}\ \gamma_{21})$; where for $z\geq h$, the SIGN$=1$; and for $z>h$, then SIGN$=-1$. The kernel matrices Θ_0 and $\Theta_j(\chi)$ ($j=1, 2, 3, 4$) are defined as follows.

$$\Theta_0=\begin{pmatrix} 0 & 0 & 0 \\ 0 & 1 & 0 \\ 0 & 0 & 0 \end{pmatrix}$$

$$\Theta_1(\chi)=\begin{pmatrix} A_1(\chi) & 0 & A_2(\chi) \\ 0 & 0 & 0 \\ -A_2(\chi) & 0 & A_3(\chi) \end{pmatrix}$$

$$\Theta_2(\chi)=\begin{pmatrix} -A_4(\chi) & 0 & -A_5(\chi) \\ 0 & 0 & 0 \\ A_6(\chi) & 0 & -A_7(\chi) \end{pmatrix}$$

$$\Theta_3(\chi)=\begin{pmatrix} -A_4(\chi) & 0 & -A_6(\chi) \\ 0 & 0 & 0 \\ A_5(\chi) & 0 & -A_7(\chi) \end{pmatrix}$$

$$\Theta_4(\chi)=A_8(\chi)\begin{pmatrix} \chi & 0 & 1 \\ 0 & 0 & 0 \\ -1 & 0 & \frac{-1}{\chi} \end{pmatrix} \tag{A1}$$

where the elements $A_j(\chi)$ ($j=1, 2, 3, 4, 5, 6, 7, 8$) are defined as follows.

$$A_1(\chi)=B_k\left(\frac{1}{c_{4k}}\chi-\frac{1}{c_{3k}\chi}\right),\qquad A_2(\chi)=B_k\left(\frac{c_{2k}+c_{4k}}{c_{3k}c_{4k}}\right)$$

$$A_3(\chi)=B_k\left(\frac{1}{c_{3k}}\chi-\frac{c_{1k}}{c_{3k}c_{4k}\chi}\right),\qquad A_4(\chi)=B_k\left(\chi^2+\frac{c_{2k}}{c_{3k}}\right)$$

$$A_5(\chi)=B_k\left(\chi+\frac{c_2k}{c_{3k}\chi}\right),\qquad A_6(\chi)=B_k\left(\frac{c_{2k}}{c_{3k}}\chi+\frac{c_{1k}}{c_{3k}\chi}\right)$$

$$A_7(\chi)=B_k\left(\chi^2+\frac{c_{2k}^2+c_{2k}c_{4k}-c_{1k}c_{3k}}{c_{3k}c_{4k}}\right),\qquad A_8(\chi)=B_k\left(c_{1k}-\frac{c_{2k}^2}{c_{3k}}\right) \tag{A2}$$

where $B_k=\frac{1}{\gamma_{1k}^2-\gamma_{2k}^2}$: for $\chi=\pm\gamma_{n1}(n=1, 2)$, then the subscript $k=1$, and for $\chi=-\gamma_{n2}$, then the subscript $k=2$.

The 7 constant square matrices in Eq. (8) are given exactly as follows: $P_{01}=\frac{1}{c_{41}\gamma_{01}}\Theta_0$, $P_{1k}=-(\gamma_{11}+\gamma_{21})M_k\Theta_1(-\gamma_{11})$, $P_{2k}=(\gamma_{11}+\gamma_{21})M_k\Theta_1(-\gamma_{21})$, $Q_1=-(\gamma_{11}+\gamma_{21})M_3\Theta_1(-\gamma_{11})$, $Q_2=(\gamma_{11}+\gamma_{21})M_3\Theta_1(-\gamma_{21})$; where $k=1, 2$; and $M_j(j=1, 2, 3)$ are defined as follows:

$$M_1=\begin{pmatrix} q_{11} & 0 & q_{13} \\ 0 & 0 & 0 \\ q_{21} & 0 & q_{23} \end{pmatrix},\ M_2=\begin{pmatrix} q_{41} & 0 & q_{43} \\ 0 & 0 & 0 \\ q_{21} & 0 & q_{23} \end{pmatrix},\ M_3=\begin{pmatrix} 0 & 0 & 0 \\ 0 & 0 & 0 \\ q_{31} & 0 & q_{33} \end{pmatrix} \tag{A3}$$

The elements in ($A3$) are given as follows.

$$q_{11}=\frac{1}{D}\left[\gamma_{11}+\gamma_{21}+\frac{(c_{41}+\sqrt{c_{11}c_{31}})(c_{12}c_{32}-c_{22}^2)}{c_{31}c_{41}\sqrt{c_{12}c_{32}}(\gamma_{21}+\gamma_{22})}\right]$$

$$q_{13}=\frac{1}{D}\left[1-\frac{c_{21}}{\sqrt{c_{11}c_{31}}}\right]$$

$$q_{21}=\frac{1}{D}\left[\sqrt{\frac{c_{11}}{c_{31}}}-\frac{c_{21}}{c_{31}}\right]$$

$$q_{23}=\frac{1}{D}[\gamma_{11}+\gamma_{21}]$$

$$q_{31}=\frac{1}{D}\left[\frac{(c_{12}c_{32}-c_{22}^2)(\sqrt{c_{11}c_{31}}-c_{21})}{c_{31}\sqrt{c_{12}c_{32}}(\gamma_{21}+\gamma_{22})}\right]$$

$$q_{33}=\frac{1}{D}\left[\frac{c_{12}c_{32}-c_{22}^2)(\gamma_{11}+\gamma_{21})}{\sqrt{c_{12}c_{32}}(\gamma_{21}+\gamma_{22})}\right]$$

$$q_{41}=\frac{1}{D}\left[\frac{(c_{22}-\sqrt{c_{12}c_{32}})(\sqrt{c_{11}c_{31}}-c_{21})}{c_{31}\sqrt{c_{12}c_{32}}(\gamma_{21}+\gamma_{22})}\right]$$

$$q_{43}=\frac{1}{D}\left[\frac{(c_{22}-\sqrt{c_{12}c_{32}})(\gamma_{11}+\gamma_{21})}{\sqrt{c_{12}c_{32}}(\gamma_{21}+\gamma_{22})}\right]$$

$$D=\left(\frac{1}{c_{41}}+\frac{1}{\sqrt{c_{11}c_{31}}}\right)\left[c_{11}-\frac{c_{21}^2}{c_{31}}+\frac{\sqrt{c_{11}}(c_{12}c_{32}-c_{22}^2)(\gamma_{11}+\gamma_{21})}{\sqrt{c_{31}c_{12}c_{32}}(\gamma_{21}+\gamma_{22})}\right] \tag{A4}$$

Appendix B

For the point force vector, the functions $g_{\alpha ij}(z)$ ($\alpha=0$; $0\leq i+j\leq 3$) are given by

$$g_{000}(z)=\frac{1}{R}$$

$$g_{010}(z)=\frac{-x}{RR_z}$$

$$g_{001}(z)=\frac{-y}{RR_z}$$

$$g_{011}(z)=\frac{-xy}{RR_z^2}$$

$$g_{002}(z)=\frac{1}{R_z}\left[1-\frac{y^2}{RR_z}\right]$$

$$g_{020}(z)=\frac{1}{R_z}\left[1-\frac{x^2}{RR_z}\right]$$

$$g_{021}(z)=\frac{y}{2R_z^2}\left[\frac{2x^2}{RR_z}-1\right]$$

$$g_{012}(z)=\frac{x}{2R_z^2}\left[\frac{2y^2}{RR_z}-1\right]$$

$$g_{003}(z)=\frac{y}{2Rz^2}\left[\frac{2y^2}{RR_z}-3\right]$$

$$g_{030}(z)=\frac{x}{2R_z^2}\left[\frac{2x^2}{RR_z}-3\right] \tag{B1}$$

where $R=\sqrt{x^2+y^2+z^2}$ and $R_z=R+z$. For $\alpha\geq 1$, the functions $g_{\alpha ij}(z)$ can be obtained by using the following transfer formula,

$$g_{\alpha ij}(z) = -\frac{\partial g_{(\alpha-1)ij}(z)}{\partial z}. \tag{B2}$$

For the ring for force vector, the functions $q_{\alpha ij}(z)$ ($\alpha=0$; $i=0, 1$; $j=0, 1$) are given by (see Eason, *et al.* 1955).

$$\begin{aligned}
q_{000}(z) &= \frac{1}{\pi}\frac{2}{R_1}K(\kappa) \\
q_{001}(z) &= \frac{-z}{\pi a R_1}\left[K(\kappa)+\frac{a-r}{a+r}\Pi(\kappa_1, \kappa)\right]+\frac{1}{a}H(a-r) \\
q_{010}(z) &= \frac{-z}{\pi r R_1}\left[K(\kappa)+\frac{r-a}{r+a}\Pi(\kappa_1, \kappa)\right]+\frac{1}{r}H(r-a) \\
q_{011}(z) &= \frac{1}{\pi}\frac{1}{arR_1}\left[R_2^2K(\kappa)-R_1^2E(\kappa)\right]
\end{aligned} \tag{B3}$$

where $\kappa_1=\frac{2\sqrt{ar}}{a+r}$, $\kappa=\frac{2\sqrt{ar}}{R_1}$, $R_1=\sqrt{(a+r)^2+z^2}$, $R_2=\sqrt{r^2+a^2+z^2}$, $K(\kappa)$, $E(\kappa)$, and $\Pi(\kappa_1, \kappa)$ are the complete elliptic integrals of the first, second, and third kinds; $H(\ )$ is the Heaviside step function. For $\alpha \geq 1$, the functions $q_{\alpha ij}(z)$ can be obtained by using the following transfer formula,

$$q_{\alpha ij}(z) = -\frac{\partial q_{(\alpha-1)ij}(z)}{\partial z} \tag{B4}$$